Phytomedicine 124 (2024) 155296

Contents lists available at ScienceDirect

Phytomedicine

journal homepage: www.elsevier.com/locate/phymed

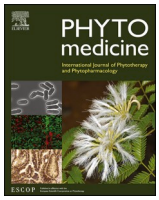

Baicalin ameliorates insulin resistance and regulates hepatic glucose metabolism via activating insulin signaling pathway in obese pre-diabetic mice

Lingchao Miao [a,#], Xutao Zhang [a,#], Haolin Zhang [a], Meng Sam Cheong [a], Xiaojia Chen [a], Mohamed A. Farag [c], Wai San Cheang [a,*], Jianbo Xiao [b,*]

[a] State Key Laboratory of Quality Research in Chinese Medicine, Institute of Chinese Medical Sciences, University of Macau, Macau SAR, China
[b] Universidade de Vigo, Nutrition and Bromatology Group, Department of Analytical and Food Chemistry, Faculty of Sciences, Ourense 32004, Spain
[c] Pharmacognosy Department, Faculty of Pharmacy, Cairo University, Cairo, Egypt

ARTICLE INFO

Keywords:
Baicalin
Diabetes mellitus
Obesity
Insulin resistance
Glucose metabolism

ABSTRACT

Background: Diabetes belongs to the most prevalent metabolic diseases worldwide, which is featured with insulin resistance, closely associated with obesity and urgently needs to be treated. Baicalin, belonging to natural flavonoids, has been reported to inhibit oxidative stress or inflammatoin.

Purpose: This study investigated the properties of baicalin on modulating abnormal glucolipid metabolism, as well as the underlying *in-vitro* and *in-vivo* mechanisms.

Methods: Insulin-resistant (IR)-HepG2 cells were stimulated by dexamethasone (20 μM) and high glucose (50 mM) for 48 h and incubated with or without baicalin or metformin for another 16 h. Male C57BL/6 J mice were fed with a high-fat diet (HFD, 60 % kcal% fat) during the total 14 weeks. Obese mice were then administered with baicalin (50 and 100 mg/kg) or vehicle solution everyday through oral gavage during the last 4-week period. Moreover, baicalin metabolisms *in vitro* and *in vivo* were determined using UPLC/MS/MS to study its metabolism situation.

Results: Exposure to dexamethasone and high glucose damaged the abilities of glycogen synthesis and glucose uptake with elevated oxidative stress and increased generation levels of advanced glycation end-products (AGEs) in HepG2 cells. These impairments were basically reversed by baicalin treatment. Four-week oral administration with baicalin ameliorated hyperglycemia and dyslipidemia in HFD-induced obese and pre-diabetic mice. Downregulation of IRS/PI3K/Akt signaling pathway accomplished with reduced GLUT4 expression and enhanced GSK-3β activity was observed in insulin resistant HepG2 cells as well as liver tissues from pre-diabetic mice; and such effect was prevented by baicalin. Moreover, baicalin and its matabolites were detected in IR-HepG2 cells and mouse plasma.

Conclusion: The study illustrated that baicalin alleviated insulin resistance by activating insulin signaling pathways and inhibiting oxidative stress and AGEs production, revealing the potential of baicalin to be a therapeutic natural flavonoid against hepatic insulin and glucose-lipid metabolic disturbance in pre-diabetes accompanied with obesity.

Abbreviations: AGEs, Advanced glycation end products; ALT, Alanine transaminase; AST, Aspartate transaminase; DXMS, Dexamethasone; DIO, Diet-induced obese; FFAs, Free fatty acids; GLUT4, Glucose transporter protein 4; GSK-3β, Glycogen synthase kinase-3β; HDL-c, High density lipoprotein cholesterol; IRS-1 and IRS-2, Insulin receptor substrates 1 and 2; IR, Insulin resistant; ITT, Insulin tolerance test; GSH, L-Glutathione; LDL-c, Low density lipoprotein cholesterol; MDA, malondialdehyde; NAFLD, Nonalcoholic fatty liver diseases; OGTT, Oral glucose tolerance test; PI3K, Phosphatidylinositol 3-kinase; Akt, Protein kinase B; PDK1, Pyruvate dehydrogenase kinase isozyme 1; ROS, Reactive oxygen species; SOD, Superoxide dismutase; TC, Total cholesterol; TG, Total triglyceride; T2DM, Type 2 diabetes mellitus.

* Corresponding authors.
E-mail addresses: annacheang@um.edu.mo (W.S. Cheang), jianboxiao@uvigo.es (J. Xiao).
Lingchao Miao and Xutao Zhang contribute equally to the work.

https://doi.org/10.1016/j.phymed.2023.155296
Received 5 June 2023; Received in revised form 12 December 2023; Accepted 16 December 2023
Available online 17 December 2023

Introduction

Type 2 diabetes mellitus (T2DM), a metabolic disease complicatedly caused by insulin resistance, is often featured with hyperlipidemia and hyperglycemia (Grundy, 2004). Under the prolonged condition of hyperglycemia, pancreatic β-cells largely increase compensatory insulin secretion, which might ultimately lead to impaired sensitivity to insulin and thereby attenuate insulin-mediated biological responses in its target tissues such as adipose tissues, liver and skeletal muscle (Petersen and Shulman, 2018; Shrivastava et al., 2021; Wen et al., 2022). Through gluconeogenesis and glycogenesis, liver plays an essential role in maintaining dynamic balance of blood sugar. Furthermore, liver regulates lipid metabolism. With T2DM and obesity, the accumulation of triglycerides in liver tissue mostly relies on free fatty acids (FFAs) recirculation from the pool of adipose tissue (Marchesini et al., 2008). Excess and long-term exposure of FFAs will result in hepatic injury and is also responsible for insulin resistance as well as blockage of insulin-mediated suppression of lipolysis (Marra et al., 2008). Ultimately, glucolipotoxicity during diabetes causes advanced glycation end products (AGEs) production and reactive oxygen species (ROS) generation in liver, which further accelerates the pathological progressions of hepatic insulin resistance and liver diseases (Giannini et al., 1999).

Once completing the joint with insulin receptor, insulin would activate a serious of complicated signaling cascades to modulate glucose uptake and metabolism. As the dominant substrate insulin receptor proteins, insulin receptor substrates 1 & 2 (IRS-1 & 2) would activate phosphatidylinositol 3-kinase (PI3K) upon binding with insulin (Shah et al., 2004). In liver metabolisms, IRS-1 is more compactly associated with maintaining glucose homeostasis while IRS-2 is more compactly related with lipids' metabolism, which play the complementary roles for each other (Taniguchi et al., 2005). After binding to pyruvate dehydrogenase kinase isozyme 1 (PDK1), PI3K would phosphorylat protein kinase B (Akt) to activate it (Sarbassov et al., 2005). Along the signaling pathway, Akt makes glycogen synthase kinase-3β (GSK-3β) phosphorylated in cytoplasm and let it deactivated (Mora et al., 2005). Importantly, glucose transporter protein 4 (GLUT4) is translocated to the cell surface of insulin-sensitive cells in response to insulin secretion, facilitating glucose uptake of the insulin-responsive tissues (Bryant et al., 2002). Furthermore, GLUT4 trafficking is also controlled by Akt in mediating insulin signaling to regulate glucose output in liver tissues (Huang and Czech, 2007).

As traditional Chinese medicine, *Scutellaria radix* roots are commonly adopted to treat and prevent T2DM, hypertension, atherosclerosis, dysentery, hyperlipidemia, and other respiratory diseases (Liao et al., 2014; Miao et al., 2022). Baicalin (7-glucuronic acid, 5, 6-dihydroxyflavone) and the aglycone form are the major active ingredients of *Scutellaria baicalensis* (Zhao et al., 2016). The anti-diabetic properties of baicalin were reported previously but potential mechanisms remain elusive. In present study, we examined and hypothesized that baicalin ameliorates insulin resistance and glucolipotoxicity in insulin resistant (IR)-HepG2 cells and high-fat diet-induced obese (DIO) mice through activating insulin signaling pathways and suppressing oxidative stress and AGEs levels.

Materials and methods

Insulin resistant HepG2 cell model

Human HepG2 cell line (SCSP-510) was got from Chinese Academy of Sciences (Shanghai, China). For cell culture, low glucose DMEM medium (Gibco, America) supplemented with 100 mg/l streptomycin and 50 U/ml penicillin and 10 % FBS (Gibco, America). HepG2 cells were stimulated by dexamethasone (DXMS) (Sigma-Aldrich, America, 20 μM) and high-glucose (Sigma-Aldrich, 50 mM) for 48 h to induce insulin resistance as previously described (Miao et al., 2023). After stimulation, baicalin (>90.0 %(T), CAS: 21967-41-9; TCI (Shanghai) Chemical Industrial Development Co., LTD) was added for another 16-h treatment.

Animal experiments

C57BL/6 J mice (male, 18–22 g) were obtained from Animal Centre in University of Macau. The animal registration number is UMARE-015–2022 and approval date is 26th July 2022. All mice were fed at 22–25° centigrade in a 12-hour light/dark cycle. Mice at 6 weeks old were set into 3 groups randomly: Control mice group, diet-induced obese (DIO) mice group, and DIO mice with baicalin administration group. DIO mice were fed a high-fat diet (HFD, 60 % kcal% fat; Shuyishuer Bio, Changzhou, China) for a total 14-week period for a pre-diabetic mouse model establishment. Control mice were fed with a chow diet. Mice of treatment group were orally administered with baicalin (50 and 100 mg/kg/day, using 0.5 % carboxymethyl cellulose sodium as the vechile solution) whilst mice in control or DIO groups were given vehicle solution during last 4 weeks.

Cell viability by MTT assay

After seeding in 96-well plates (5~6 × 10^3 cells/well), in model group, HepG2 cells were stimulated by 20 μM DXMS and 50 mM d-glucose for 48 h with control group cells cultured with low glucose DMEM medium. Then, cells were treated with a 16-h incubation with baicalin (25 and 50 μM) or metformin (2 mM). The absorbance (OD) data were obtained at 490 nm.

Glucose uptake assay

After high glucose plus DXMS induction with or without baicalin treatment, metformin was given as the positive control, glucose uptake kit (RongSheng Biotech, Shanghai, China) was adopted to detect the glucose consumption capacity of HepG2 cells according to protocol, OD values were measured at 505 nm.

Intracellular glycogen levels assay

Glycogen test kit (Bioengineering Institute of Nanjing Jiancheng, Jiangsu, China) was performed according to protocol. After chromogenic reaction, OD results were acquired at 620 nm. The total concentrations of intracellular glycogen in different groups of HepG2 cells were obtained according to the conversion.

Intracellular ROS generation levels assay

DCFH-DA probe, obtained from Beyotime Biotechnology company (Shanghai, China) was used to measure the intracellular ROS levels of HepG2 cells. After drug treatments, intracellular fluorescence intensity was detected in cells using a flow cytometry (Beckman Coulter, America) immediately during 45 min. The intracellular ROS levels were also measured by a DMI8 inverted fluorescent microscope (Leica, Germany). The experimental protocol was same as previous described (Miao et al., 2023).

Determination of AGEs

AGEs levels in cells, plasma and livers were measured according to kit's instructions (Bioengineering Institute of Nanjing Jiancheng). The absorbance results were obtained at 450 nm immediately within 10 min. AGEs production levels were calculated according to the computational formula using Origin 9.1 (America).

Western blotting analysis

HepG2 cells and liver tissues of mice were added with RIPA solution

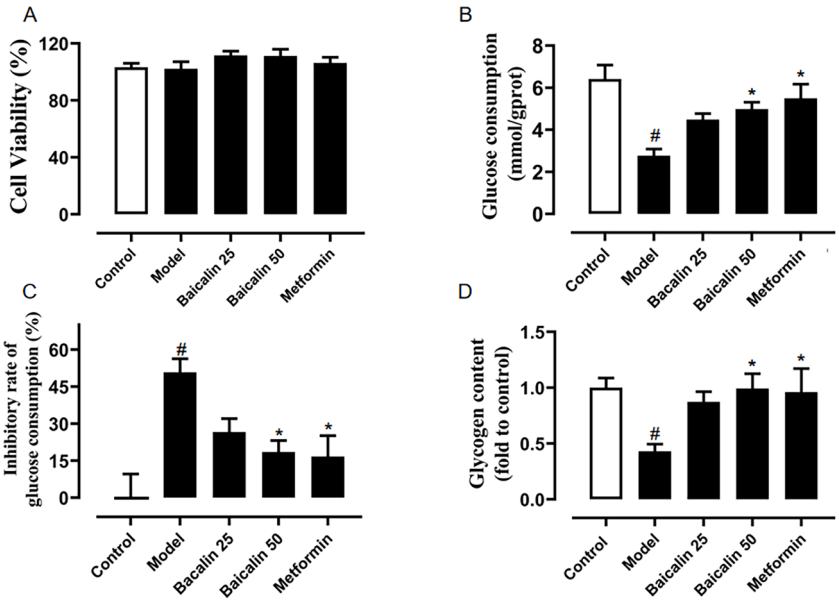

Fig. 1. Baicalin improves glucose uptake and glycogen synthesis in insulin resistant (IR)-HepG2 cells. (A) Cell viability of HepG2 cells induced by 50 mM HG and 20 μM DXMS for 48 h (model), followed by 25 μM and 50 μM baicalin treatment for another 16 h. Metformin (2 mM) was chosen as positive control. The results were expressed as% to control group. (B) Glucose uptake content of control and IR-HepG2 cells which were treated with blank medium, 2 mM metformin or baicalin (25 μM and 50 μM) for another 16 h. (C) Inhibitory rate of glucose uptake in IR-HepG2 cells as normalized to control. (D) Intracellular glycogen content of IR-HepG2 cells treated with 25 μM and 50 μM baicalin or 2 mM metformin for 16 h compared with control group. Data are presented as the mean ± SEM ($n = 5$). #$p < 0.05$ vs Control, *$p < 0.05$ vs Model.

(Beyotime) for lysis. The protein concentrations of samples were detected by BCA assay. Samples were stacked followed by separation using 8∼10 % SDS/PAGE gels. Then, blots were electrophoretically transferred into PVDF membranes under an ice bath condition. After that, membranes were blocked at room temperature for 2 h by 5 % defatted milk TBST buffer. Then, membranes were incubated by corresponding primary antibodies for 18–20 h at 4 °C. After washed by TBST, membranes were probed with secondary antibodies for 2 h. Anti-IRS-2, GAPDH, Akt, GSK-3β, *phospho*-Akt (Ser473) and *phospho*-GSK-3β (Ser9) primary antibodies, and secondary antibodies were acquired from Cell Signaling Technology (Beverly, USA). PI3K primary antibody was bought from Proteintech (Wuhan, China) whereas IRS-1 and GLUT4 were from Abcam (Cambridge, UK). Ultimately, membranes were visualized by BIO-RAD Imaging System (America), analyzed by BIO-RAD Image Lab Touch Software (America).

Measurement of blood glucose level

In oral glucose tolerance test (OGTT), mice were orally administrated with glucose solution (1.2 g glucose/kg body weight) after a 6-h fasting, and blood glucose levels were measured at time intervals of 0, 15, 30, 60 and 120 min by a commercial glucometer (Yuwell, Jiangsu, China). In insulin tolerance test (ITT), after 2-h fasting, mice were injected with 0.5 U insulin/kg mouse body weight i.p. Blood glucose levels were obtained at same time intervals of 0, 15, 30, 60 and 120 min.

Biochemical analysis in plasma and liver

Plasma samples were taken to detect insulin levels, low and high density lipoprotein cholesterol (LDL-c & HDL-c), total cholesterol (TC) and total triglyceride (TG) by assay kits (Bioengineering Institute of Nanjing Jiancheng). Levels of aspartate transaminase (AST), HDL-c, LDL-c, alanine transaminase (ALT), superoxide dismutase (SOD), l-Glutathione (GSH) and malondialdehyde (MDA) in mice liver tissues were measured according to kits manufacturers' instructions.

Histological analysis

Mouse liver were fixed in 10% formaldehyde solution. Liver samples were then embedded in paraffin and sliced into sections (10 μm) stained with hematoxylin-eosin (H&E) (Beyotime Biotechnology). Oil red reagent was adopted to stain the sections to observe the lipid distribution, visualizing nuclei using hematoxylin (Beyotime Biotechnology). Images were photographed at × 400 magnification by an optical microscope.

Metabolism analysis of baicalin in vitro and in vivo

Plasma samples of control C57 BL/6 J mice were collected at time points of 0, 1, 3, 5, 7, and 12 h after oral administration with 100 mg/kg body weight baicalin. Sample was added with methanol (containing 0.1 % formic acid) and swirled for 2 min and then centrifuged at 12,000 rpm for 10 min to get supernatant. Afterwards, samples were examined using a Thermo UltiMate 3000 UHPLC system with a Thermo Scientific LTQ Orbitrap XL hybrid FT Mass Spectrometer (San Jose, CA, USA). To achieve the chromatographic separation, a ACQUITY UPLC HSS T3 column (1.8 μm, 2.1 × 150 mm) and a ACQUITY UPLC BEH C18 column (2.1 × 50 mm, 1.7 μm) (Waters Technology, America) were used. The mobile phases as 0.1% formic acid in water (solvent A) and acetonitrile (solvent B) were taken as 0.3 ml/ min flow rate. HepG2 cell and plasma samples from C57BL/6 J mice were injected and eluted by gradient elution method. The MS full scans were obtained from m/z 80 to 1 500 with a 30 000 mass resolution. Xcalibur software (Thermo Scientific, USA) was taken to collect and analyze results.

Statistical analysis

Data were represented as mean ± SEM to acquire the representative results. GraphPad Prism 8, Origin 9 and Image-Pro-Plus 6.0 (USA) were used. Apart from this, multiple comparisons between or among the experimental groups were distinguished by T-test, one-way or two-way ANOVA. Significant difference was indicated when p value was < 0.05.

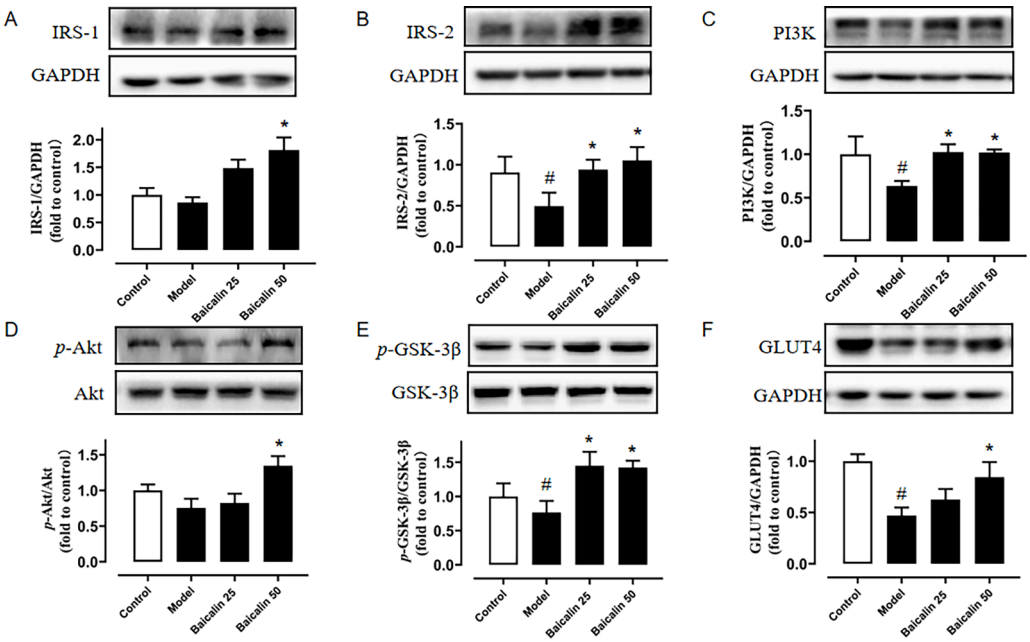

Fig. 2. Baicalin regulates insulin signaling in IR-HepG-2 cells. Western blots showing expression levels of (A) IRS-1 and (B) IRS-2 compared to GAPDH, (C) PI3K compared to GAPDH, (D) Ser473 phosphorylated and total Akt, (E) phosphorylation at Ser9 and total GSK-3β, and (F) GLUT4 compared to GAPDH, in HepG2 cells stimulated with high glucose (50 mM) plus DXMS (20 μM) and treated with baicalin (25 μM and 50 μM). Data are mean ± SEM ($n = 3$). #$p < 0.05$ vs Control; *$p < 0.05$ vs Model.

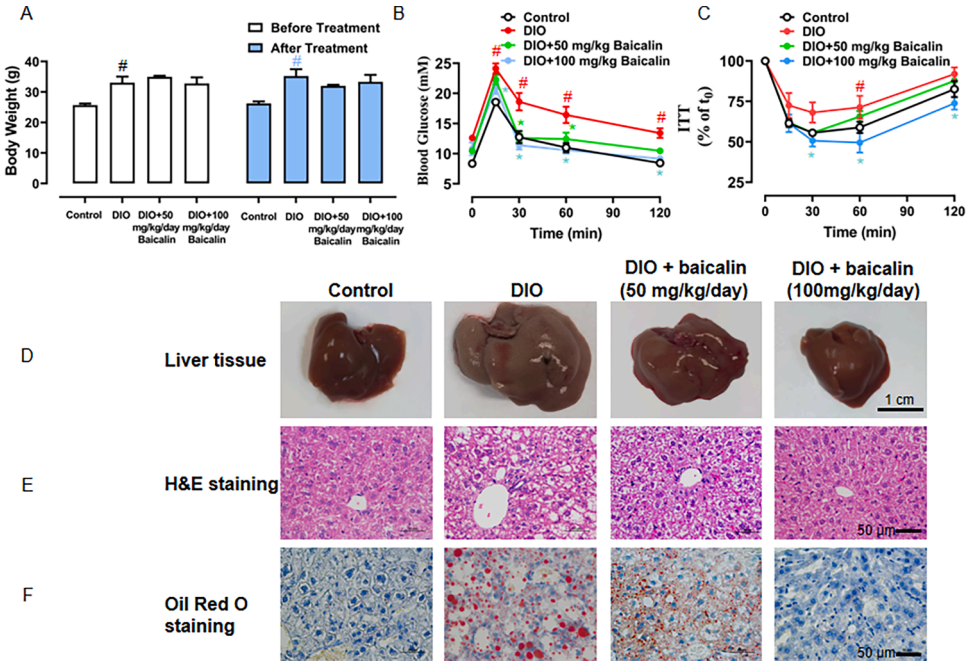

Fig. 3. Protective function of baicalin in diabetic and obese mice. (A) Body weight changes in mice fed with standard chow diet or high-fat diet for total 14 weeks and orally administered with vehicle (0.25 % CMC—Na solution) or baicalin (50 and 100 mg/kg/day) during the last 4 weeks. (B) Oral glucose tolerance test (OGTT) results upon 6-h fasting. (C) Insulin tolerance test (ITT) results upon 2-h fasting. (D) Representative images of liver tissues in mice. (E-F) Representative H&E staining and Oil red O staining images of mouse liver sections (scale bar at 50 μm). Data are mean ± SEM ($n = 4$–5). #$p < 0.05$ vs Control; *$p < 0.05$ vs DIO.

Results

Baicalin improves glucose uptake and glycogen synthesis in IR-HepG2 cells

25 μM and 50 μM were confirmed as non-toxic baicalin concentrations, as well as 2 mM of metformin to IR-HepG2 cells via MTT assay (Fig. 1**A**), which were chosen in the following cell experiments. After stimulation of high glucose (HG, 50 mM) and DXMS (20 μM), IR-HepG2 cells consumed glucose concentration decreased almost a half, as compared with control group. Glucose uptake ability of insulin resistant HepG2 cells was recovered by baicalin treatment especially at higher concentration of 50 μM significantly, achieving similar results to metformin (Fig. 1**B and C**). As shown in Fig. 2**D**, intracellular synthesized glycogen in HepG2 cells were remarkably reduced by DXMS and HG

Table 1
Lipid profile, insulin level and hepatic function index of male C57BL/6 J mice on normal (control) or high-fat diet (DIO) with or without baicalin treatment. Data are means ± SEM of 4–5 experiments. #$p<0.05$ vs control; *$p<0.05$ vs DIO.

Plasma levels of	Control	DIO	DIO + Baicalin
Total cholesterol (mg/dl)	126.60 ±4.96	205.30±7.09 #	166.00±18.20 *
Triglycerides (mg/dl)	91.56 ±11.57	142.60±2.44 #	133.60±1.74*
HDL (mM)	3.56±0.15	4.69±0.37	5.93±0.51
LDL (mM)	0.91±0.07	2.49±0.15 #	1.62±0.04 *
AST (IU/l)	14.18±4.93	183.20±19.55 #	96.42±27.12
ALT (IU/l)	159.20 ±3.24	189.40±8.93 #	136.50±9.99 *
Insulin (mIU/l)	2.17±0.54	0.43±0.11 #	1.55±0.51 *
Liver tissue levels of	Control	DIO	DIO + Baicalin
HDL (mmoL/gprot)	0.079±0.004	0.053±0.007 #	0.088±0.004 *
LDL (mmoL/gprot)	0.029±0.001	0.050±0.012	0.035±0.009
AST (U/gprot)	40.44±1.19	86.27±18.63 #	57.27±0.95
ALT (U/gprot)	42.44±1.16	64.28±1.03 #	51.66±2.31 *

stimulation, which was reversed by 25 and 50 μM baicalin and 2 mM metformin treatment.

Baicalin activates IRS/PI3K/Akt signaling in insulin resistant HepG2 cells

The expression levels of IRS-2 and PI3K decreased obviously after HG and DXMS stimulation, while baicalin enhanced them significantly at both 25 μM and 50 μM (Fig. 2**B and C**). By contrast, IRS-1 and Ser473 *phospho*-Akt were mildly but not apparently suppressed in IR-HepG2 cells; these levels were remarkably upregulated by baicalin at 50 μM (Fig. 2**A and D**). Baicalin also alleviated suppressions of phosphorylated GSK-3β at Ser9 and GLUT4 in DXMS and HG induced IR-HepG2 cells (Fig. 2**E-F**). Phosphorylation of GSK-3β at Ser9 is inhibitory for its kinase activity.

Four-week oral administration of baicalin improves glucose and lipid metabolism in DIO mice

Shown as Fig. 3**A**, body weight of mice fed with high-fat diet increased apparently compared to control mice fed with chow diet either before or after baicalin treatment. The body weight of obese mice were similar upon vehicle or baicalin administration. Baicalin treatment (both 50 and 100 mg/kg/day) remarkably improved glucose tolerance deteriorated in DIO mice (Fig. 3**B**). For modulating insulin sensitivity, higher oral concentraion of baicalin at 100 mg/kg/day obviously exhibited better therapeutic effect with significance (Fig. 3**C**).

The size of DIO mouse liver tissue was much bigger than that of lean control mouse. Not only that, DIO mouse liver tissue was pale and full of distinct fat particles compared with lean control mouse, while baicalin treatment (100 mg/kg/day better than 50 mg/kg/day) significantly improved these histopathological aberrant traits (Fig. 3**D**). As shown in liver sections from DIO mice, hepatocytes were loosely arranged, and their structures turned to be cloudy swelling featured with cytoplasm vacuolization compared with control mice. Baicalin treatment at 100 mg/kg/day restored these histopathological transformations in liver tissues more apparently than lower concentration at 50 mg/kg/day (Fig. 3**E**). Liver sections stained by Oil red O illustrated that baicalin treatment (100 mg/kg/day) significantly decreased hepatic lipids accumulation of DIO mice, improving hepatic steatosis (Fig. 3**F**). Moreover, DIO mice had suffered from hyperlipidemia and liver injury manifested by increased levels of TC, LDL, AST, TG and ALT in plasma and liver tissues compared with control mice; and such impairments were ameliorated by baicalin treatment (Table 1). In addition, baicalin treatment increased HDL levels in DIO mice liver tissues significantly and slightly decreased DIO mice plasma insulin levels (Table 1).

Baicalin ameliorates pre-diabetes through activating insulin signaling pathways in DIO mice

Expression levels of IRS-1, PI3K, IRS-2, and Ser473 *phospho*-Akt were all down-regulated in liver tissues of DIO mice but could be increased by

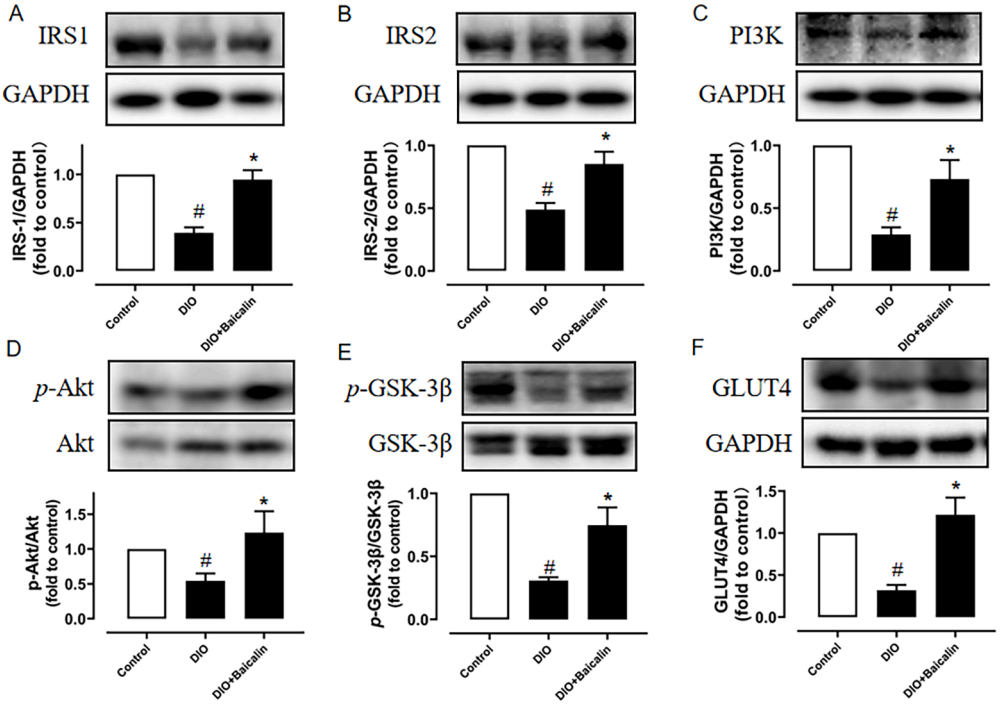

Fig. 4. Baicalin chronic treatment activates insulin signaling pathways in DIO mice. Western blotting data showing expression levels of (A) IRS-1 and (B) IRS-2 compared to GAPDH, (C) PI3K compared to GAPDH, (D) Ser473 phosphorylation of Akt compared to total Akt, (E) Ser9 phosphorylation of GSK-3β compared to total GSK-3β and (F) GLUT4 compared to GAPDH in liver tissues. Data are mean ± SEM of 4–5 experiments. #$p<$ 0.05 vs Control; *$p<$ 0.05 vs DIO.

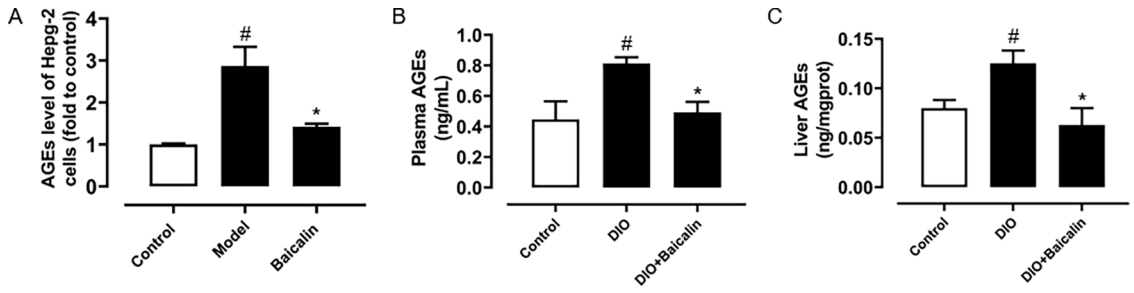

Fig. 5. Effect of baicalin on AGEs levels. (A) Intracellular AGEs levels in HepG2 cells induced by 50 mM high glucose and 20 μM dexamethasone (DXMS) for 48 h and treated with baicalin (50 μM) for another 16 h. (B) Plasma and (C) liver AGEs levels in control and DIO mice with 4-week oral administration of baicalin. Data are mean ± SEM (n = 3–5). #p< 0.05 vs Control, *p< 0.05 vs Model or DIO.

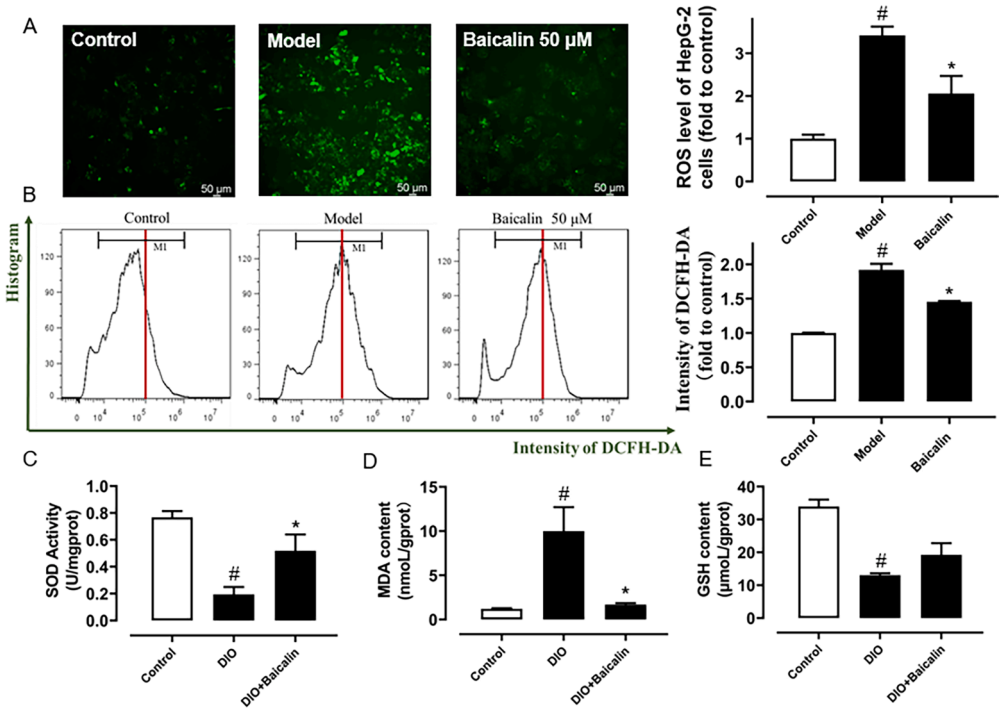

Fig. 6. Baicalin treatment suppresses oxidative stress. (A) Representative images and the summarized graph of green fluorescence (DCFH-DA probe) in HepG2 cells stimulated by 50 mM high glucose with 20 μM dexamethasone and treated with 50 μM baicalin for anther16 h. (B) Representative flow cytometry diagrams and summarized graph of intracellular ROS levels using DCFH-DA probe in IR-HepG-2 cells with same treatment as before. (C) SOD activity, (D) MDA and (E) GSH levels in liver tissues of DIO mice with 4-week oral gavage of baicalin (100 mg/kg/day). Data are the means ± SEM (n = 3–5). #p< 0.05 vs Control, *p< 0.05 vs Model or DIO.

baicalin treatment (Fig. 4**A-D**). In addition, reduction in protein expression levels of Ser9 *phospho*-GSK-3β and GLUT4 were observed in DIO mice liver tissues, comparing with that of control mice. Baicalin administration could effectively reverse the reduction in DIO mice (Fig. 4**E-F**).

Baicalin treatment suppressed AGEs levels in IR-HepG2 cells and DIO mice

To explore the effect of baicalin on AGE-ROS axis, the AGEs levels in IR-HepG2 cells and in plasma and liver tissues of 3 groups of mice were measured. AGEs levels were stimulated sharply by high glucose with DXMS *in vitro* and high-fat diet *in vivo* comparing to control whereas AGEs levels were normalized by baicalin treatment (Fig. 5).

Baicalin inhibits oxidative stress in IR-HepG2 cells and livers from DIO mice

The ROS levels were determined in IR-HepG2 cells using DCFH-DA probe under fluorescence microscope, which was significantly raised in model group and decreased efficiently with baicalin treatment (Fig. 6**A**). In line with these data, the results of flow cytometry indicated that baicalin diminished ROS levels as shown in Fig. 6**B**. Additionally, SOD activity and GSH expression levels which could reflect antioxidant capacity in liver tissues were suppressed to a great extent in DIO mice. Chronic baicalin treatment significantly enhanced SOD activity, and mildly though insignificantly increased GSH content (Fig. 6**C and E**). Not only that, MDA production also increased sharply in livers of DIO mice, which was inhibited by baicalin treatment effectively (Fig. 6**D**).

Baicalin metabolism situation in vitro and in vivo

The intracellular metabolisms of baicalin by IR-HepG2 cells after its treatment at 5 min, 30 min and 16 h comparing to the model group were studied. Histogram intensity of baicalin and its methylated form (m/z = 461.11) increased significantly during 5 min to 30 min in cells. Yet, after 16-h treatment, very little baicalin and its methylated form could be

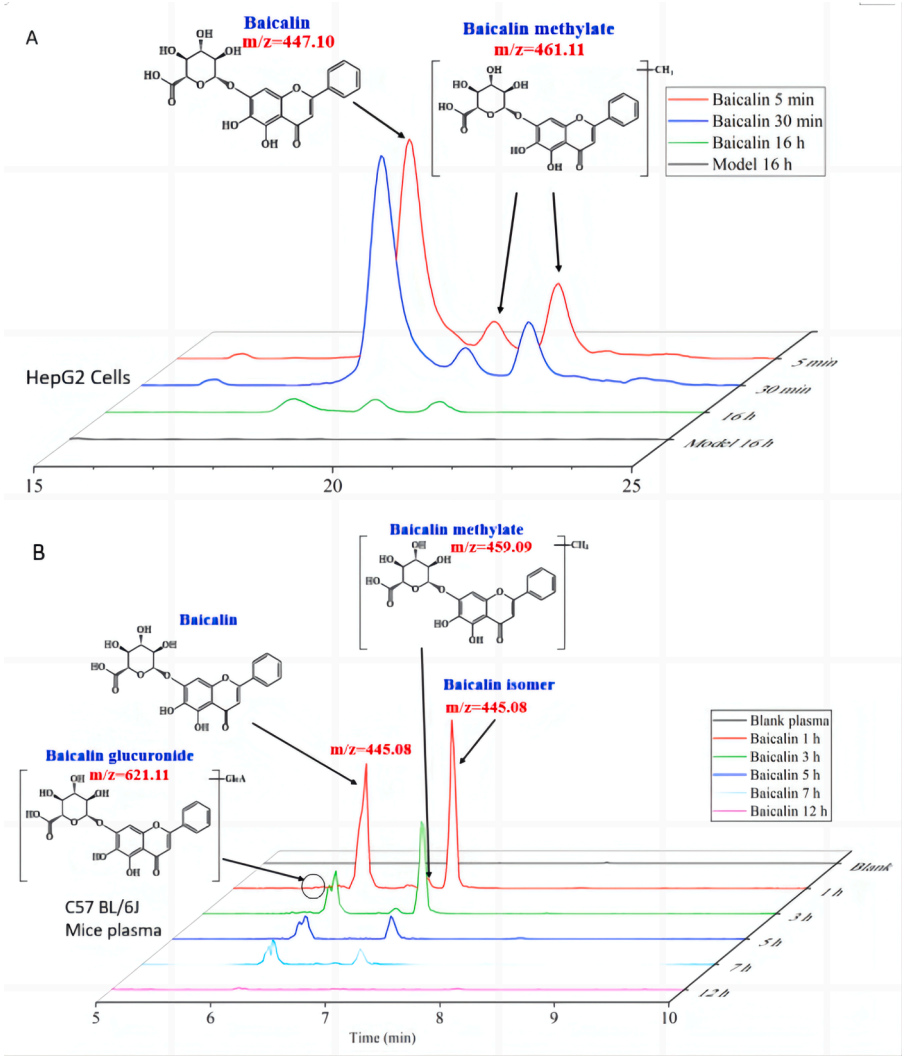

Fig. 7. Identified metabolites of baicalin in HepG2 cells and plasma of C57BL/6 J mice. (A) Extracted ion chromatograms (EIC) of $m/z = 447.10$ (Baicalin) and $m/z = 461.11$ (Baicalin methylate) at positive ion mode from HepG2 cell samples. (B) EIC of $m/z = 445.08$ (Baicalin and its isomer), $m/z = 459.09$ (Baicalin methylate), $m/z = 621.11$ (Baicalin glucuronide) at negative ion mode from mouse plasma samples.

detected (Fig. 7**A**). Baicalin metabolism was examined in plasma samples from C57BL/6 J mice. After oral administration with 100 mg/kg baicalin, the plasma levels of baicalin and its isomer ($m/z = 445.08$) reached relatively high at the first hour, and gradually dropped but held up pretty well till 7 h. Moreover, methylate ($m/z = 459.09$) and glucuronide ($m/z = 621.11$) of baicalin were found at the first hour (Fig. 7**B**). After a 12-h process, baicalin and its metabolites almost all disappeared in mouse blood.

Discussion

In our present study, the results suggested that effect of baicalin on treating pre-diabetes in IR-HepG2 cells and DIO pre-diabetic mice was owing to improving hepatic insulin resistance, disordered glucose and lipid metabolism via activating insulin signaling pathways, associated with significant suppression on ROS and AGEs. Besides, metabolism situation of baicalin at different time points *in vitro* and *in vivo* was investigated to better understand its biological activities.

Baicalin has been reported to be protective against diabetes and its complications. Baicalin exhibits anti-diabetic effect on streptozotocin (STZ)-induced diabetic Wistar rats by upregulating hepatic glycogen content and glycolysis, protecting mitochondrial membrane, and thereby improving antioxidant status (Li et al., 2011). Moreover, baicalin has been described to improve obesity-related disorders and hepatic steatosis via activating hepatic AMP activated protein kinase (AMPK) and acetyl-CoA carboxylase (ACC) in rodents fed with high-fat diet (Xi et al., 2015). Furthermore, 8-week oral treatment of baicalin improves diabetic nephropathy via decreasing proteinuria, renal histopathological changes and cell apoptosis in male db/db mice. The potential mechanisms involves inhibition on the inflammatory infiltration, mRNA levels of pro-inflammatory cytokines (IL-1β, IL-6, MCP-1 and TNF-α) as well as activation on Nrf2/HO-1/NQO1 signaling pathway (Ma et al., 2021). The aforementioned published studies use db/db mice or STZ injection to create diabetic models and have found that baicalin treatment exhibits decent anti-diabetic effect. Herein, we adopted the diet-induced obese mice model, which is widely considered as an obese and insulin resistant, kind of pre-diabetic model. We are first to illustrate that baicalin could alleviate hepatic insulin resistance, disordered glucose-lipid metabolism, and fatty liver via activation of IRS/PI3K/Akt insulin signaling pathways with up-regulation of GLUT4 and inhibition of GSK-3β activity in pre-diabetes and obesity through *in vitro* and *in vivo* assays. Furthermore, the improvement of pre-diabetes and obesity by baicalin might be attributed to its suppression on oxidative stress, AGEs production and hepatic abnormal lipid accumulation.

Liver, as one of the major organs governing whole-body metabolism, modulates glucose and lipid homeostasis (Postic et al., 2004). Once liver

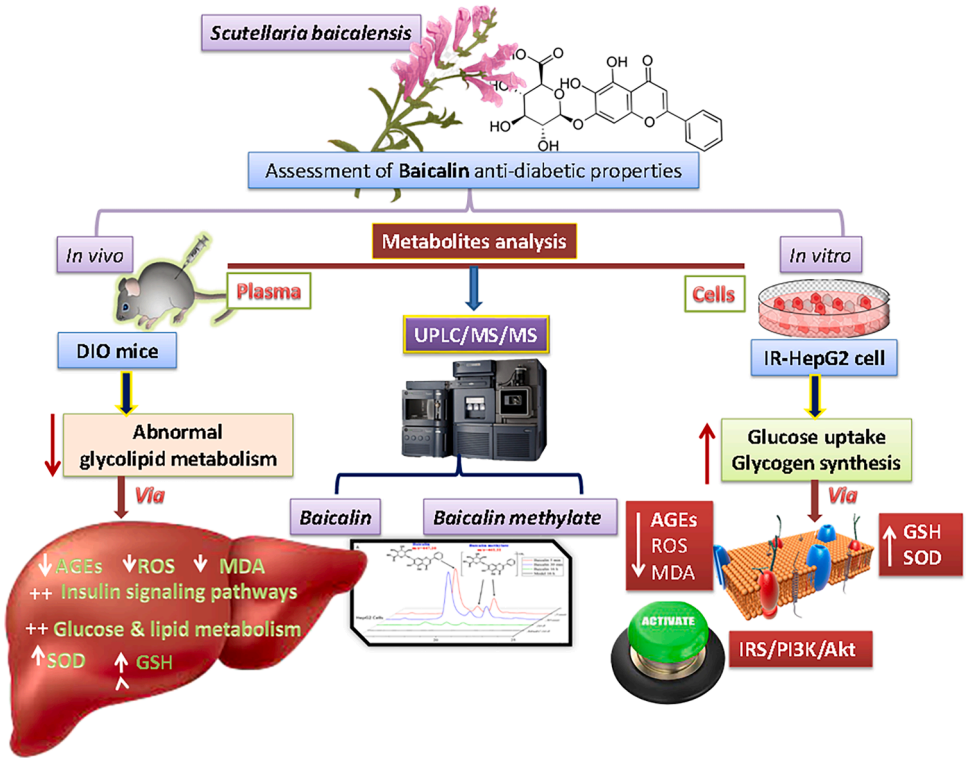

Fig. 8. Summarized graph for the present study.

energy metabolism like glucose uptake or glycogen synthesis is disturbed, harmful responses will be resulted, such as diabetes, insulin resistance, and nonalcoholic fatty liver diseases (NAFLD) (Birkenfeld and Shulman, 2014; Tilg et al., 2017). In current study, hepatic glucose uptake and glycogen synthesis abilities damaged by high glucose were improved by baicalin *in vitro* with efficacy similar to metformin. Moreover, disordered insulin sensitivity, glucose tolerance as well as pathological AST or ALT levels and fatty liver were all alleviated by chronic baicalin treatment especially at higher oral concentration of 100 mg/kg/day in DIO mice. These findings are in agreement with previous studies.

In liver, adipose tissue and skeletal muscle, these insulin-responsive tissues, glucose metabolism is regulated by insulin through binding to IRS-1 and 2, which further recruit PI3K and activate Akt (Gammeltoft and Van Obberghen, 1986; Vanhaesebroeck et al., 2010). Akt-dependent GSK-3β phosphorylation could contribute to glycogen synthase activation and thus elevated glucose storage as glycogen (Manning and Cantley, 2007). Under insulin resistant conditions, *phospho*-GSK-3β is inhibited, further inhibiting glycogen synthesis. Our novel findings supported that baicalin at higher oral concentration 100 mg/kg/day ameliorated hepatic insulin resistance and pre-diabetes through activating insulin signaling pathways *in vivo* and *in vitro*, up-regulating IRS/PI3K/Akt/GLUT4 pathway and inhibiting GSK-3β activity.

Excessive generations of ROS and AGEs are closely associated with diabetes progression featured with hyperglycemia, and they are regarded as pivotal markers of diabetes and obesity (Luc et al., 2019). ROS over-accumulation under disturbed redox homeostasis caused by obesity and hyperglycemia results in oxidative stress and signaling cascades activation that aggravate diabetic pathology and diabetes-related complications (Ha et al., 2008; Kaneto et al., 2010). Accompanied with oxidative stress, the irreversible AGEs formation through intracellular glycation aggravates diabetes pathology (Yamagishi et al., 2012). Present study illustrated that baicalin could inhibit AGEs and ROS levels significantly, which likely contribute to its anti-diabetic effect.

Of note, baicalin metabolic changes were investigated by UPLC/MS/MS. Data of the intracellular and plasma metabolites could better understand the pharmacological activities of baicalin. Baicalin was absorbed by HepG2 cells or into the bloodstream of C57BL/6 J mice and was then metabolized into glucuronide and methylated products to exhibit pharmacological functions *in vitro* and *in vivo*. Besides, the presence of baicalin and its metabolism were confirmed in hepatocytes. The results implied that baicalin consumed orally could be absorbed into the bloodstream and get into liver cells to exert its effect on ameliorating insulin resistance and regulating hepatic glucose metabolism via activating insulin signaling pathways. However, which metabolites including baicalin methylate and baicalin glucuronide and their efficacy to mediate the effects on improving pre-diabetes and lipids disorder at different time-points after administration should be further investigated in the future through pharmacokinetics-pharmacodynamics (PK-PD) or toxicological studies of baicalin for further development.

Conclusions

To conclude (Fig. 8), present study showed that pre-diabetes could be ameliorated by baicalin through improving glycogen synthesis and glucose consumption abilities through activation of insulin signaling pathway and inhibiting ROS and AGEs production. Moreover, baicalin ameliorated dyslipidemia and liver injury associated with diabetes. The relelation of the present study highlights the promising theraputic potential of baicalin in hepatic insulin resistance in pre-diabetes and obesity.

CRediT authorship contribution statement

Lingchao Miao: Investigation, Methodology, Writing – original draft. **Xutao Zhang:** Investigation, Methodology. **Haolin Zhang:** Investigation, Methodology. **Meng Sam Cheong:** Data curation. **Xiaojia Chen:** Validation. **Mohamed A. Farag:** Writing – review & editing. **Wai San Cheang:** Supervision, Writing – review & editing. **Jianbo Xiao:**

Supervision, Writing – review & editing.

Declaration of Competing Interest

The authors declare that they have no known competing financial interests or personal relationships that could have appeared to influence the work reported in this paper.

Acknowledgments

This research was funded by the Science and Technology Development Fund, Macau SAR (SKL-QRCM(UM)−2023–2025), Ramón y Cajal grant (RYC2020–030365-I) and Xunta de Galicia for supporting the program (Excelencia-ED431F2022/01).

References

Birkenfeld, A.L., Shulman, G.I., 2014. Nonalcoholic fatty liver disease, hepatic insulin resistance, and type 2 diabetes. Hepatology 59, 713–723.
Bryant, N.J., Govers, R., James, D.E., 2002. Regulated transport of the glucose transporter GLUT4. Nat. Rev. Mol. Cell Biol. 3, 267–277.
Gammeltoft, S., Van Obberghen, E., 1986. Protein kinase activity of the insulin receptor. Biochem. J. 235, 1–11.
Giannini, E., Botta, F., Fasoli, A., Ceppa, P., Risso, D., Lantieri, P.B., Celle, G., Testa, R., 1999. Progressive liver functional impairment is associated with an increase in AST/ALT ratio. Dig. Dis. Sci. 44, 1249–1253.
Grundy, S.M., 2004. Obesity, metabolic syndrome, and cardiovascular disease. J Clin. Endocrinol. Metab. 89, 2595–2600.
Ha, H., Hwang, I.A., Park, J.H., Lee, H.B., 2008. Role of reactive oxygen species in the pathogenesis of diabetic nephropathy. Diabetes Res. Clin. Pract. 82 (Suppl 1), S42–S45.
Huang, S., Czech, M.P., 2007. The GLUT4 glucose transporter. Cell Metab. 5, 237–252.
Kaneto, H., Katakami, N., Matsuhisa, M., Matsuoka, T.A., 2010. Role of reactive oxygen species in the progression of type 2 diabetes and atherosclerosis. Mediat. Inflamm. 2010, 453892.
Li, H.T., Wu, X.D., Davey, A.K., Wang, J., 2011. Antihyperglycemic effects of baicalin on streptozotocin - nicotinamide induced diabetic rats. Phytother. Res. 25, 189–194.
Liao, P., Liu, L., Wang, B., Li, W., Fang, X., Guan, S., 2014. Baicalin and geniposide attenuate atherosclerosis involving lipids regulation and immunoregulation in ApoE-/- mice. Eur. J. Pharmacol. 740, 488–495.
Luc, K., Schramm-Luc, A., Guzik, T.J., Mikolajczyk, T.P., 2019. Oxidative stress and inflammatory markers in prediabetes and diabetes. J. Physiol. Pharmacol. 70.
Ma, L., Wu, F., Shao, Q., Chen, G., Xu, L., Lu, F., 2021. Baicalin Alleviates Oxidative Stress and Inflammation in Diabetic Nephropathy via Nrf2 and MAPK Signaling Pathway. Drug Des. Dev. Ther. 15, 3207–3221.
Manning, B.D., Cantley, L.C., 2007. AKT/PKB signaling: navigating downstream. Cell 129, 1261–1274.
Marchesini, G., Moscatiello, S., Di Domizio, S., Forlani, G., 2008. Obesity-associated liver disease. J. Clin. Endocrinol. Metab. 93, S74–S80.
Marra, F., Gastaldelli, A., Svegliati Baroni, G., Tell, G., Tiribelli, C., 2008. Molecular basis and mechanisms of progression of non-alcoholic steatohepatitis. Trends Mol. Med. 14, 72–81.
Miao, L., Liu, C., Cheong, M.S., Zhong, R., Tan, Y., Rengasamy, K.R.R., Leung, S.W.S., Cheang, W.S., Xiao, J., 2022. Exploration of natural flavones' bioactivity and bioavailability in chronic inflammation induced-type-2 diabetes mellitus. Crit. Rev. Food Sci. Nutr. 1–28.
Miao, L.C., Zhang, H.L., Cheong, M.S., Zhong, R.T., Garcia-Oliveira, P., Prieto, M.A., Cheng, K.W., Wang, M.F., Cao, H., Nie, S.P., Simal-Gandara, J., San Cheang, W., Xiao, J.B., 2023. Anti-diabetic potential of apigenin, luteolin, and baicalein via partially activating PI3K/Akt/GLUT-4 signaling pathways in insulin-resistant HepG2 cells. Food. Sci. Hum. Wellness 12, 1991–2000.
Mora, A., Sakamoto, K., McManus, E.J., Alessi, D.R., 2005. Role of the PDK1-PKB-GSK3 pathway in regulating glycogen synthase and glucose uptake in the heart. FEBS Lett. 579, 3632–3638.
Petersen, M.C., Shulman, G.I., 2018. Mechanisms of insulin action and insulin resistance. Physiol. Rev. 98, 2133–2223.
Postic, C., Dentin, R., Girard, J., 2004. Role of the liver in the control of carbohydrate and lipid homeostasis. Diabetes Metab. 30, 398–408.
Sarbassov, D.D., Guertin, D.A., Ali, S.M., Sabatini, D.M., 2005. Phosphorylation and regulation of Akt/PKB by the rictor-mTOR complex. Science 307, 1098–1101.
Shah, O.J., Wang, Z., Hunter, T., 2004. Inappropriate activation of the TSC/Rheb/mTOR/S6K cassette induces IRS1/2 depletion, insulin resistance, and cell survival deficiencies. Curr. Biol. 14, 1650–1656.
Shrivastava, A.K., Thapa, S., Shrestha, L., Mehta, R.K., Gupta, A., Koirala, N., 2021. Phytochemical screening and the effect of Trichosanthes dioica in high-fat diet induced atherosclerosis in Wistar rats. Food Frontiers 2, 527–536.
Taniguchi, C.M., Ueki, K., Kahn, R., 2005. Complementary roles of IRS-1 and IRS-2 in the hepatic regulation of metabolism. J. Clin. Investig. 115, 718–727.
Tilg, H., Moschen, A.R., Roden, M., 2017. NAFLD and diabetes mellitus. Nat. Rev. Gastroenterol. Hepatol. 14, 32–42.
Vanhaesebroeck, B., Guillermet-Guibert, J., Graupera, M., Bilanges, B., 2010. The emerging mechanisms of isoform-specific PI3K signalling. Nat. Rev. Mol. Cell Biol. 11, 329–341.
Wen, Y., Liu, Y., Huang, Q., Farag, M.A., Li, X, Wan, X., Zhao, C., 2022. Nutritional assessment models for diabetes and aging. Food Frontiers 3, 689–705.
Xi, Y., Wu, M., Li, H., Dong, S., Luo, E., Gu, M., Shen, X., Jiang, Y., Liu, Y., Liu, H., 2015. Baicalin attenuates high fat diet-induced obesity and liver dysfunction: dose-response and potential role of CaMKKβ/AMPK/ACC pathway. Cell. Physiol. Biochem. 35, 2349–2359.
Yamagishi, S., Maeda, S., Matsui, T., Ueda, S., Fukami, K., Okuda, S., 2012. Role of advanced glycation end products (AGEs) and oxidative stress in vascular complications in diabetes. Biochim. Biophys. Acta 1820, 663–671.
Zhao, Q., Chen, X.Y., Martin, C., 2016. Scutellaria baicalensis, the golden herb from the garden of Chinese medicinal plants. Sci. Bull. 61, 1391–1398.